Journal of Engineering Physics and Thermophysics, Vol. 74, No. 5, 2001

CONDENSATION WAKE IN A NONISOBARIC JET

A. N. Kucherov and G. V. Molleson UDC 536.6+536.42

We demonstrate the substantial effect of the nonisobaricity of an exhaust jet on the initial parameters of a condensation wake: distance to the wake, initial water content, ice content, optical thickness, and transverse dimension.

The interest in investigating physical processes in condensation wakes (contrails) has increased with increase in ejections from aircraft to the atmosphere that affect the ozone, CO_2, and aerosols, including high cirrus clouds [1–5]. A contrail behind a large passenger airplane (B-747-400, IL-96, etc.) is formed at altitudes of 8–14 km near the tropopause in a jet regime of exhaust [3], at distances of $\sim 10^1$–10^2 m from the nozzle. The physical model involves the following assumptions: the jet is isobaric and the flight velocity and the parameters of the exhaust gas across the nozzle cut are constant [6, 7]. In [8] it is shown that the initial parameters of a contrail change substantially (~100%) at relatively small (~10%) variations in temperature or moisture content at the nozzle cut and also during seasonal-latitudinal changes in the atmospheric conditions. In the present work, we investigate the effect of the nonisobaricity of a jet on the initial characteristics of a contrail.

We place the origin of a cylindrical coordinate system (x, r) at the center of the cut of a nozzle of radius r_a. The pressure in this section differs N times from the atmospheric one, $p_a = Np_\infty$. We consider the hot section of the equalization of pressure ($(p - p_\infty)/p_\infty \le 1\%$) near the nozzle $\Delta x \le 10 r_a$ and evaluate the change in the temperature and velocity of the gas. Thereafter, we investigate the turbulent diffusion of the jet and cooling and condensation (crystallization) of water vapor. Condensation begins in the cold peripheral region. At a certain distance x_m from the nozzle, the aerosol converges on the axis. By the initial section x_m, the transverse optical thickness $\tau(x;\ \lambda) = \int_0^\infty \alpha(x, r; \lambda) dr$ increases sharply up to the maximum and then decreases [9]. The quantity α is the coefficient of the attenuation of radiation by aerosol at the wavelength λ.

The jet is described by the Euler or Navier–Stokes equations near the nozzle and by the equations of turbulent expansion of the type of the Prandtl boundary-layer equation:

$$\frac{\partial \rho u r}{\partial x} + \frac{\partial \rho v r}{\partial r} = 0 \; ; \tag{1}$$

$$\frac{\partial \rho u^2}{\partial x} + \frac{1}{r}\frac{\partial \rho u v r}{\partial r} + \frac{1}{\kappa M_\infty^2}\frac{\partial p}{\partial x} = \frac{1}{r}\frac{\partial}{\partial r}\left\{\frac{r\mu}{\mathrm{Re}}\frac{\partial u}{\partial r}\right\}, \; p_{\mathrm{phys}} = \rho_{\mathrm{phys}} T_{\mathrm{phys}} \frac{R}{m}, \quad \mathrm{Re} = \frac{\rho_\infty u_\infty r_a}{\mu_a} \; ; \tag{2}$$

N. E. Zhukovskii Central Aerohydrodynamic Institute, Zhukovskii, Russia; email: ank@dept.aerocentr.msk.su. Translated from Inzhenerno-Fizicheskii Zhurnal, Vol. 74, No. 5, pp. 29–32, September–October, 2001. Original article submitted October 17, 2000.

 1062-0125/01/7405-1090$25.00

$$\frac{\partial \rho u v}{\partial x}+\frac{1}{r}\frac{\partial \rho v^2 r}{\partial r}+\frac{1}{\kappa M_\infty^2}\frac{\partial p}{\partial r}\approx 0\,,\quad M_\infty^2=\frac{u_\infty^2\rho_\infty}{\kappa p_\infty}\,; \tag{3}$$

$$\frac{\partial \rho u H}{\partial x}+\frac{1}{r}\frac{\partial \rho v r H}{\partial r}=\frac{1}{r}\frac{\partial}{\partial r}\left\{\frac{r\mu}{\mathrm{Pr\,Re}}\frac{\partial H}{\partial r}\right\},\quad H_{\mathrm{phys}}=C_pT_{\mathrm{phys}}+\frac{u_{\mathrm{phys}}^2+v_{\mathrm{phys}}^2}{2}\,,\quad \mathrm{Pr}=\frac{C_p\mu_{\mathrm{a}}}{k_{\mathrm{a}}}\,; \tag{4}$$

$$\frac{\partial \rho u Y}{\partial x}+\frac{1}{r}\frac{\partial \rho v r Y}{\partial r}=\frac{1}{r}\frac{\partial}{\partial r}\left\{\frac{r\mu}{\mathrm{Sc\,Re}}\frac{\partial Y}{\partial r}\right\},\quad Y=\frac{\rho_{\mathrm{v}}}{\rho}\,,\quad \mathrm{Sc}=\frac{\mu_{\mathrm{a}}}{\rho_\infty D_{\mathrm{a}}}\,; \tag{5}$$

$$\text{for }\; x=0\,,\quad 0\le r\le 1:\; u=U\equiv\frac{u_{\mathrm{a}}}{u_\infty}\,,\quad v=0\,,\quad T=A_T\equiv\frac{T_{\mathrm{a}}}{T_\infty}\,,\quad p=N\,,\quad \rho=\frac{N}{A_T}\,,\quad Y=Y_{\mathrm{a}}\,; \tag{6}$$

$$\text{for }\; x=x_{\min}\,,\quad 1\le r\le r_{\max}:\; u=1\,,\quad v=0\,,\quad T=1\,,\quad p=1\,,\quad \rho=1\,,\quad Y=Y_\infty\,; \tag{7}$$

$$\text{for }\; r=0\,,\quad r=r_{\max}\,,\quad x_{\min}\le x\le x_{\max}:\; \frac{\partial u}{\partial r}=0\,,\quad v=0\,,\quad \frac{\partial T}{\partial r}=0\,,\quad \frac{\partial p}{\partial r}=0\,,\quad \frac{\partial \rho}{\partial r}=0\,,\quad \frac{\partial Y}{\partial r}=0\,. \tag{8}$$

Here ρ, u, v, p, and T are related to the parameters in the cocurrent flow ρ_∞, u_∞, p_∞, and T_∞; the coordinates x and r are related to r_{a}, the coefficients μ, k, and D to the characteristic values μ_{a}, k_{a}, and D_{a}; u_{a} and T_{a} are the velocity and temperature at the nozzle cut; R is the universal gas constant; C_p and m are the heat capacity at constant pressure and molar mass of the exhaust mixture ($\approx$ air); the similarity numbers are: the Mach (M_∞), Reynolds (Re), Prandtl (Pr), and Schmidt (Sc) numbers; κ is the specific heat ratio; N is the inefficiency ratio (nonisobaricity) parameter; Y_∞ and Y_{a} are the mass concentration of vapor in the atmosphere and at the nozzle cut; $u_\infty/u_{\mathrm{a}} = 1/U$ is the flow cocurrency; $A_T = T_{\mathrm{a}}/T_\infty$ is the parameter of heating; the quantities $x_{\min}$, $x_{\max}$, and $r_{\max}$ denote the maximum and minimum dimensions of the computational domain.

In the computational regime $N = 1$ in a cruising flight (9–13 km) the Mach number at the nozzle cut $M_{\mathrm{a}} = M_\infty U/\sqrt{A_T}$ is close to unity and the parameters U and A_T are equal to 1.5–2.5. In [10] the parameters at the nozzle cut of the engine in a B-747-400 airplane are given: $r_{\mathrm{a}} = 1.1$ m; for $0\le r\le r_{\mathrm{a}}/2$, $u = 437$ m/sec, $T = 590$ K, and the mole fraction of vapor is 0.00428; for $r = r_{\mathrm{a}}/2$, $u = 316$ m/sec and $T = 284$ K; in the atmosphere $u_\infty = 237$ m/sec, $p_\infty = 23{,}900$ N/m^2 (10.7 km), and $T_\infty = 219$ K. We approximate the temperature and velocity profiles by a smooth function equal to the sum of three Gaussian functions of the arguments, r/r_{a}, $(1 - 2r/r_{\mathrm{a}})$, and $(1 - r/r_{\mathrm{a}})$. With the constancy of mass flows and of the total gas enthalpy H_{a}:

$$\rho_{\mathrm{a}}u_{\mathrm{a}}=\rho_{\mathrm{a}N}u_{\mathrm{a}N}\,,\quad \rho_{\mathrm{a}}u_{\mathrm{a}}H_{\mathrm{a}}=\rho_{\mathrm{a}N}u_{\mathrm{a}N}H_{\mathrm{a}N}\,,\quad \rho_{\mathrm{va}}u_{\mathrm{a}}=\rho_{\mathrm{va}N}\,u_{\mathrm{a}N} \tag{9}$$

the equivalent uniform distribution has velocity $u_{\mathrm{a}} = 396$ m/sec ($U = 1.67$), temperature $T_{\mathrm{a}} = 465$ K ($A_T = 2.12$), and density of the mixture $\rho_{\mathrm{a}} = 0.179$ kg/m^3 and of the vapor $\rho_{\mathrm{va}} = 0.00306$ kg/m^3 ($Y_{\mathrm{a}} = 0.0017$). The effect of the initial transverse distributions is not taken into account here.

We consider two nonisobaric regimes.

I. According to Eq. (9), the gas and vapor flow rate and the total enthalpy at the nozzle cut and the fuel flow rate are preserved. The parameters U_N, A_{TN}, and $Y_{\mathrm{a}N}$ are related to the inefficiency ratio parameter N via the relation

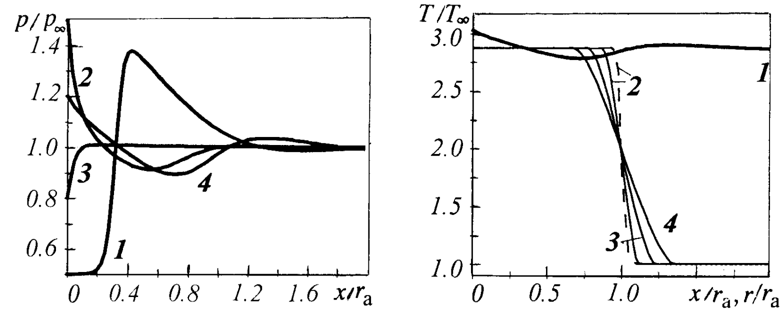

Fig. 1. Pressure along the axis $p(x, 0)/p_\infty$: 1) N = 0.5 (variant I); 2) 1.5 (I); 3) 0.8 (II); 4) 1.2 (II) and the temperature along the axis $T(x, 0)/T_\infty$ (curve 1) and across the axis (without account for 2) $T(x = 4r_a, r)$ (dashed curve) and with account for viscosity and heat capacity (solid curves) 2) $T(x = 4r_a, r)$, 3) $T(x = 8r_a, r$; 4) $T(x = 12r_a, r)$).

$$U_N = f(N)\, U\,,\quad A_{TN} = Nf(N)\, A_T\,,\quad Y_{aN} = Y_a\, f(N)\,,\quad f = \frac{NC_pT_a}{u_a}\left[\sqrt{1 + \frac{2u_a^2 H_a}{(NC_pT_a)^2}} - 1\right]; \tag{10}$$

II. The Mach number at the nozzle cut is kept constant, $M_{aN} \equiv M_\infty U_N/\sqrt{A_{TN}} = M_\infty U/\sqrt{A_T} \equiv M_a(\approx 0.917)$, due to the change in the flow rate of fuel Δq_f and of the supplied energy $E_f\Delta q_f$:

$$\rho_a u_a\,(1+\varepsilon) = \rho_{aN}u_{aN}\,,\quad \rho_a u_a\,(H_a + \varepsilon E_f) = \rho_{aN}u_{aN}H_{aN}\,,\quad \rho_{va}u_a + \varepsilon\rho_a u_a E_w = \rho_{vaN}u_{aN}\,,$$

$$\frac{u_a}{\sqrt{T_a}} = \frac{u_{aN}}{\sqrt{T_{aN}}}\,,\quad N = \frac{\rho_{aN}T_{aN}}{\rho_a T_a}\,,\quad \varepsilon = \frac{\Delta q_f}{\rho_a u_a} = \left(\frac{1}{2} + \frac{H_a}{2E_f}\right)\left[\sqrt{1 + \frac{4\,(N^2-1)\,H_a/E_f}{(1 + H_a/E_f)^2}} - 1\right], \tag{11}$$

$$U_N = \frac{N}{1+\varepsilon}\,U\,,\quad A_{TN} = \left(\frac{N}{1+\varepsilon}\right)^2 A_T\,,\quad Y_{aN} = \frac{Y_a + \varepsilon E_w}{1+\varepsilon}\,.$$

Here E_f (= 43 MJ/kg, kerosene) is the caloric power of a fuel and E_w (= 1.25 kg/kg of fuel) is the index of water emission.

It was noted in [11] that the transverse pressure gradients are equalized at distances $\Delta x < r_a$. In the section of longitudinal pressure equalization $p_e(x_e) \approx p_\infty$ (the subscript e means "equilibrium"), a good approximation for calculating the corresponding parameters ρ_e, u_e, r_e, and T_e is given by the formulas of adiabatic (H = const) and isoentropic (p/ρ^κ = const) expansion [11, 12] that are written in the form

$$\frac{1}{N} = \frac{p_e}{p_{aN}} = \left(\frac{\rho_e}{\rho_{aN}}\right)^\kappa = \left(\frac{T_e}{T_{aN}}\right)^{\frac{\kappa}{\kappa-1}}\,,\quad \frac{T_e}{T_{aN}} = N^{-\frac{\kappa-1}{\kappa}}\,,\quad \frac{\rho_e}{\rho_{aN}} = N^{-\frac{1}{\kappa}}\,,$$

$$\frac{u_e}{u_{aN}} = \frac{M_e\sqrt{T_e}}{M_{aN}\sqrt{T_{aN}}}\,,\quad \frac{r_e}{r_{aN}} = \sqrt{\frac{\rho_{aN}u_{aN}}{\rho_e u_e}}\,,\quad Y_e = Y_{aN}\,,\quad M_e = \sqrt{N^{\frac{\kappa-1}{\kappa}}\left(\frac{2}{\kappa-1} + M_{aN}^2\right) - \frac{2}{\kappa-1}}\,. \tag{12}$$

For the evaluation of the distance of the equalization of the pressure, effect of viscosity, heat conduction, and diffusion on homogeneous transverse distributions of the parameters and for the evaluation of the error of Eq.

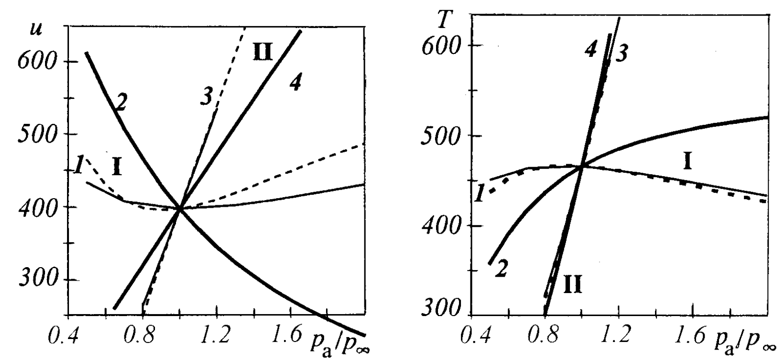

Fig. 2. The velocity u_e in the isobaric sections [1, 3) $u_e(x/r_a = 12.3, r = 0]$; dashed curves, according to formulas (12); 2, 4) u_{aN}; 1, 2) variant I with a variable M_{aN}, 3, 4) variant II, M_{aN} = const and the temperature T_e and T_{aN} as functions of the parameter $N = p_a/p_\infty$ (notation is the same). u, m/sec; T, K.

(12), numerical solutions were obtained by the method of large particles [13] over the starting length $-2 \le x/r_a \le 12$, $0 \le r/r_a \le 2.5$ within the framework of the Euler and Navier–Stokes equations on the grid $N_x = 522$, $N_r = 150$. Here N_x and N_r are the number of nodes in the direction of the coordinates x and r, respectively. Figure 1 demonstrates the dependences of the pressure p at the axis on the coordinate x and the transverse distributions of the temperature T with account for the viscosity and thermal conductivity and without it. When $x/r_a > 3$, the pressure differs from the atmospheric one by less than 1%. The temperature and velocity of the jet attain stationary levels. The effect of viscosity and thermal conductivity on the transverse distributions of velocity and temperature at distances $x/r_a < 4$ can be neglected. Dissipative processes at short distances do not exert an effect on the pressure distributions and the velocity and temperature levels in the section of the atmospheric pressure development.

In Fig. 2 the values of velocity u_e and temperature T_e from Eq. (12) are compared with numerical results in the range of the jet inefficiency ratio $0.5 < N < 2$ for two variants I and II of the change in the parameters at the nozzle cut with a variable and constant Mach number M_{aN}. Only for the velocity at the edges of the considered range of the parameter N do the values of u_e calculated from formulas (12) differ markedly from numerical ones (by up to 10%). Condensation primarily experiences the effect of changes in the temperature. Thus, the nonisobaricity of the jet can be taken into account by simple conversion into equivalent values of the temperature, velocity, and density in the section of equalization of the pressure by formulas (12).

The calculation of the condensation (crystallization) of water vapors will be performed by well-known semi-empirical relations [12]. We also use the linearized asymptotic solutions of Eqs. (2)–(5) [14], which are valid for $x_m >> r_a$:

$$\frac{u-u_\infty}{u_e-u_\infty}=\frac{H-H_\infty}{H_e-H_\infty}=\frac{Y-Y_\infty}{Y_e-Y_\infty}=\frac{\rho_e u_e r_e^2}{\rho_\infty u_\infty R_j^2(x)}\exp\left(-\frac{r^2}{R_j^2(x)}\right), \tag{13}$$

$$R_j(x)=r_e\left(\frac{6\rho_e u_e x}{\rho_\infty u_\infty r_e \mathrm{Re}_j}\right)^{1/3}, \quad j=u,H,Y, \quad \mathrm{Re}_u=\mathrm{Re}, \quad \mathrm{Re}_H=\mathrm{Pr}\,\mathrm{Re}, \quad \mathrm{Re}_Y=\mathrm{Sc}\,\mathrm{Re}.$$

The coefficient of radiation attenuation by a polydisperse aerosol is equal [15, 16] to

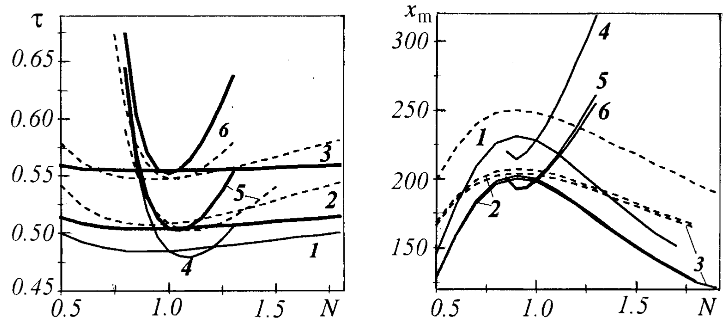

Fig. 3. The optical thickness of the jet τ [in the section of 1, 4) condensation; 2, 5) crystallization, the relative humidity $S_\infty = 0$; 3, 6) crystallization, $S_\infty = 0.9$; 1–3) variant I; 4–6) II; dashed curves, from asymptotic formulas (13), Re = 80, Pr = 0.75, Sc = 0.80] and the distance to the contrail x_m as a function of N (notation is the same). x_m, m.

$$\alpha(x, r, \lambda) = n \int_0^\infty \pi a^2 Q(a) F(a)\, da = \beta(\nu, a_{mod}, \lambda)\, w_{w,i}(x, r),$$

where n is the number density of particles, $Q(a)$ is the factor of radiation attenuation on one particle, $F(a)$ is the size distribution function of particles a, β is the specific attenuation coefficient, and $w_{w,i} = \rho Y$ is the water content or ice content of the aerosol. We select $F(a)$ in the form of the gamma-function $\Gamma(\nu)$, $\nu = 2$; the modal radius $a_{mod} \approx 1.13$ (or 5.62) μm. At the wavelength $\lambda = 10.6$ μm, the coefficient $\beta = 1.7\beta_{w,i} = 4\pi\kappa_{w,i}/\lambda\rho_{w,i} \approx 72$; 80 m^2/kg, where $\kappa_{w,i} = 0.0690$, 0.0602 and $\rho_{w,i}$ are the indices of absorption and of the density of water and ice. In the model of monodisperse aerosol of ice particles for this value of β there correspond spheres of radius $a \approx 3.3$ (or 17.0) μm or plates of thickness 1 μm.

The dependences of the distance x_m and optical thickness $\tau(x_m)$ in initial sections of condensation and crystallization and also of the distance x_m on the nonisobaricity parameter N are presented in Fig. 3. For variant I, the changes in the optical thickness in the entire considered range of the efficiency ratio $0.5 \le N \le 1.8$ are small (2–3%). The distance to the contrail x_m changes by 37–38%. The values of water content and ice content of the aerosol $w_{w,i}(x_m, 0)$ that are maximum over the section $x = x_m$ change by 15–16%; the initial (at $x = x_m$) radius of the contrail r_m changes by 8–9%. In variant II in the range $0.8 \le N \le 1.2$ the following changes are possible: in the optical thickness by 28–32%, the distances x_m by 19–25%, water (ice) content by 102–114%, and of the radii r_m by 27–36%. These estimates relate to a perfectly dry atmosphere $S_\infty \equiv \rho_{v\infty}/\rho_{v.s\infty} = 0$, where $\rho_{v.s\infty}$ is the density of a saturated vapor at the temperature T_∞. When $S_\infty = 0.9$, for a crystalline aerosol we respectively have $\Delta w_i/w_i$ = 14–15% (variant I) and 27–97% (II), $\Delta\tau/\tau$ = 0.5–1% and 7.8–12%, $\Delta x_m/x_m$ = 35–37% and 0.5–18%, and $\Delta r_m/r_m$ = 9–10% and 30–40%.

The asymptotic solution (13) (dashed curves in Fig. 3) was normalized in the crystallization section ($S_\infty = 0.9$) to the semi-empirical solution given in [12] for the calculated ($N = 1$) variant II due to the selection of the values Re = 80, Pr = 0.75, and Sc = 0.8. Here, the discrepancies in other calculated variants (1, 2 — I, 4, 5 — II) did not exceed 10%. The functions $\tau(N)$ obtained on the basis of Eq. (13) are similar for all of the variants to those obtained on the basis of the formulas from [12]. The maximum differences are close to the error of the semi-empirical solution, except for the values of x_m in variant II.

Thus, the pressure in the nonisobaric jet is equalized over short distances of the order of several radii of the nozzle. The viscosity, heat conduction, and diffusion over these distances have no time to substantially affect the transverse distributions of the parameters of the exhaust gas. Changes in the temperature and velocity in an unrated jet in comparison with an isobaric one influence the ice content and water content of the aerosol, the transverse dimension and the optical thickness in the initial section of the contrail, and on the distance to it. One should also expect a substantial effect for accelerating objects.

This work was carried out with financial support from the Russian Foundation for Basic Research (grant No. 99-01-00446) and the Central Aerodynamic Institute. We are grateful to A. A. Semenov and A. P. Markelov for a discussion of the possible situations with the efficiency ratio of the jet.

NOTATION

x and *r*, longitudinal and transverse coordinates; *N*, inefficiency ratio parameter; *p*, pressure; *T*, temperature; ρ, density; *u* and *v*, components of the velocity of the medium; *H*, enthalpy; *Y*, relative mass concentration of vapor (water drops, ice crystals); λ, radiation wavelength; τ, optical thickness of the aerosol; μ, *k*, and *D*, coefficients of turbulent dynamic viscosity, heat conduction, and diffusion. Subscripts: a, parameters at the nozzle cut averaged over the radius; ∞, parameters in the cocurrent flow; *N*, nonisobaric parameters at the nozzle cut; e, equilibrium parameters in the section of pressure equalization; f, fuel; v, vapor; S, saturated vapor; m, section of maximum optical thickness; mod, modal radius of aerosol particles; w, water; i, ice; *T*, temperature.

REFERENCES

1. K. P. Hoinka, M. E. Reinhardt, and W. Metz, *J. Geophys. Res.*, **98**, No. D12, 23113–23131 (1993).
2. O. B. Toon, R. C. Miake-Lye, *Geophys. Res. Lett.*, **25**, No. 8, 1109–1112 (1998).
3. T. Gerz, T. Dureck, and P. Konopka, *J. Geophys. Res.*, **103**, No. D20, 25905–25913 (1998).
4. O. B. Popovicheva, A. M. Starik, and O. N. Favorskii, *Izv. Ross. Akad. Nauk, Fiz. Atmosfery Okeana*, **36**, No. 2, 163–176 (2000).
5. A. N. Kucherov, *Opt. Atmosfery Okeana*, **13**, No. 5, 521–528 (2000).
6. B. Kärcher, *J. Geophys. Res.*, **100**, No. D9, 18835–18844 (1995).
7. B. Kärcher, T. Peter, U. M. Biermann, and V. Schumann, *J. Atmosph. Sci.*, **53**, No. 21, 3066–3083 (1996).
8. A. N. Kucherov, A. P. Markelov, A. A. Semenov, and A. V. Shustov, in: *Proc. V Int. Symp. "New Aviation Technologies of XXI Century,"* Sec. 1.1, 17–22 August, 1999, Zhukovsky, Russia (1999), pp. 382–389.
9. A. N. Kucherov, in: V. J. and T. A. Corcoran (eds.), *SOQUE Proc. Int. Conf. LASERS-99*, 13–17 December, 1999, Quebec, Canada, Vol. 22, USA (2000), pp. 143–150.
10. B. Kärcher, *J. Geophys. Res.*, **99**, No. D7, 14509–14517 (1994).
11. G. N. Abramovich, *Applied Gas Dynamics* [in Russian], Pt. 1, Moscow (1991).
12. V. E. Kozlov, A. N. Sekundov, and I. P. Smirnova, in: V. V. Struminskii (ed.), *Problems of Turbulent Flows* [in Russian], Moscow (1987), pp. 171–177.
13. O. M. Belotserkovskii and Yu. M. Davydov, *Method of Large Particles in Gas Dynamics* [in Russian], Moscow (1982).
14. É. S. Grinats, A. V. Kashevarov, and A. L. Stasenko, *Interaction of Vortices and Jets of High-Altitude Airplanes and Chemisorption of Nitrogen Oxides by Water Droplets* [in Russia], Preprint No. 81 of Central Aerohydrodynamic Institute (TsAGI), Moscow (1993).
15. C. F. Bohren and D. R. Huffman, *Absorption and Scattering of Light by Small Particles* [Russian translation], Moscow (1986).
16. V. E. Zuev, A. A. Zemlyanov, Yu. D. Kopytin, and A. P. Kuzikovskii, *Powerful Laser Radiation in Atmospheric Aerosol* [in Russian], Novosibirsk (1984).